EMITTANCE MEASUREMENTS AT THE LBNL ECR AND AECR-U ION SOURCE USING A PEPPER-POT EMITTANCE SCANNER *

M.Strohmeier[#,1,2], J.Y.Benitez[1], D.Leitner[1], D.Winklehner[1], D.S.Todd[1], C.M.Lyneis[1], M.Bantel[2]

[1] Lawrence Berkeley National Laboratory, 1 Cyclotron Road, Berkeley, CA, 94720, U.S.A.
[2] University of Applied Science Karlsruhe, Moltkestrasse 30, 76133 Karlsruhe, Germany

Abstract

Two Electron Cyclotron Resonance (ECR) ion sources are currently available to inject beams into the 88-Inch Cyclotron at Lawrence Berkeley National Lab (LBNL). Ion beam emittances for various ion species of both sources were measured using a recently commissioned pepper-pot emittance scanner[1] and are discussed in this paper. Pepper-pot scanners[1,2,3] are capable of extracting the full four-dimensional transverse phase space of the beam, allowing for the calculation of the cross coupled emittances xy' and yx'. This is especially of interest for ECR ion sources, where asymmetric beams are extracted in the presence of a strong solenoidal field. The axial field adds a rotational momentum to the extracted beam resulting in a transverse emittance growth, which depends on the magnetic stiffness of the extracted species. In this paper, the pepper-pot software is described and emittance data from both LBNL ECR sources are presented and compared. The data confirm a strong mass dependence of the normalized emittance for ions with the same mass-to-charge-state ratio, as previously also observed by other groups. This dependence indicates different particle distributions at the extraction aperture for different ion species.

INTRODUCTION

Electron cyclotron resonance (ECR) ion sources are widely used in the particle accelerator community because they are capable of producing high current beams of highly charged ions. Their operation relies on magnetically confined plasmas in which the electrons are resonantly heated with microwave radiation. They can reach energies of several hundred keV and ionize the gas in a step-by-step ionization process. In order to achieve high charge states, long confinement times (milliseconds) are needed which are achieved by the superposition of an axial mirror field and a radial multi-pole field, resulting in a minimum B-field configuration. Since the extraction aperture of most ECR sources is located near the center of the extraction solenoid coil, particles are extracted and accelerated in a decreasing magnetic field, which increaes the transverse emittance. Two different types of emittance scanners are currently in operation at LBNL to measure the beam emittance: an Allison type slit scanner[4] and a pepper-pot scanner[1]. The slit scanner can provide a better spatial and angular resolution than the pepper-pot,

but measurements take a few minutes. Additionally, the slit scanners can only extract one-dimensional data sets, since the intensities are integrated over the whole slit while stepping through the beam. Scintillator based pepper-pot scanners capture the image data in just a fraction of a second, making it less vulnerable to emittance changes caused by plasma instabilities or other transitions. Furthermore, the image array of a pepper-pot scanner provides two dimensional data sets from which the xx' and yy' as well as the cross coupled xy' and yx' phase spaces can be extracted.

The principle of the pepper-pot scanner[1,2,3] is to image the beam as it passes through a hole mask and creates a light pattern on a scintillator behind the mask. By knowing the absolute locations of the holes in the mask and relating them to the light pattern on the scintillator, one can obtain the transverse angular distribution of the particles in the ion beam. Since the pepper-pot scanner uses a camera (typically a CCD camera) to capture the light pattern on the scintillator, it is important to investigate the influence of the optical parameters on the emittance. These parameters can greatly influence the final emittance values and have to be chosen carefully in order to minimize and define the induced error stemming from the respective parameters[2]. For the scintillator, the absolute light yield, its linearity and the lattice degradation as a function of the integrated beam exposure are crucial parameters [1, 2]. Camera settings that influence the emittance value are the exposure time of the charge coupled device CCD chip to the scene, the gain and the brightness.

NOISE PROCESSING

The noise treatment consists of the following three steps, which are described in this section in detail:

1. Detecting faulty pixels.
2. Smoothing the data.
3. Threshold cut of the data.

1) Detecting fault pixels

As CCD cameras age, the pixel array degrades, and the number of faulty pixels increases. If the camera is additionally mounted in a radiation environment, this degradation is even more accelerated. Unfortunately, the gray scale values of these damaged pixels show a random distribution rather than a constant value of "255" or "0". Neglecting these pixels for the emittance evaluation would introduce a large error in the calculation. Therefore, before calculating the emittance value the analyzing software needs to locate and replace those pixels with approximated values. In order to locate the faulty pixels, a reference image without beam has to be

recorded where the faulty pixels are clearly visible. Empirically, a gray scale value of about 80 was found to be an appropriate threshold to decide which pixels are damaged. Once those pixels are identified, they are substituted in the real image with the average of the eight intermediate neighbors.

2) Smoothing the data

In the next step a 3x3 smoothing filter is applied to the data. While this simple smoothing filter turns out to work well, future tests will compare more filter types such as low-pass filters, Gaussian filters or median filters.

3) Threshold cut of the data

In the last step, a threshold cut is applied to the image with a value that can be set online via a slider on the GUI (graphical user interface) to eliminate electrical noise in the image. The GUI gives the user an immediate visual feedback of how the threshold level affects the data. The value of the threshold cut has to be chosen carefully since it is a measure of how much beam intensity is neglected and will be discussed later in this paper. Typical threshold values are in the order of 10 to 15 gray scale units (which is less than 5% of the full dynamic range). Figure 1 shows two profile plots of the same image slice before and after the noise processing steps described above were applied.

Influence of noise threshold on the emittance

In this section, the influence of the value for the threshold cut which is applied to the raw data on the obtained emittance number is discussed. The threshold cut is problematic since the "real" emittance of the beam is not known and the border regions of the spots greatly influence the obtained emittance value. By applying a threshold cut, these border regions are disregarded and the emittance becomes artificially smaller. The neglected portion of the beamlet increases with the value for that threshold cut. The black curve in Figure 1 shows that without a threshold cut, the beamlets cannot be separated, which is essential for the pepper-pot evaluation software[1].
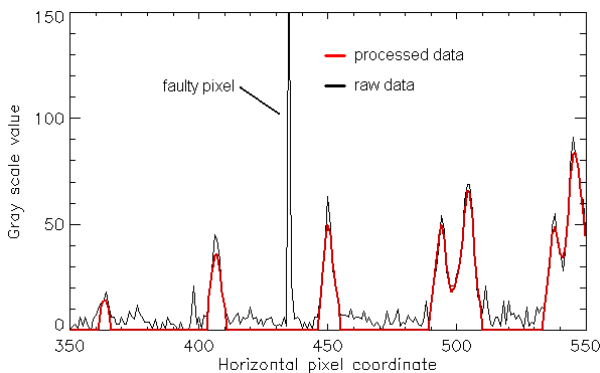

Figure 1: Plot of the same image slice before and after the noise processing steps were applied. BLACK: raw data, RED: after eliminating the faulty pixels, smoothing and thresholding the data.

Curve-fitting to each of the spots would eventually make the threshold cut obsolete; this software improvement will be implemented in the future. Figure 2 shows the emittance curves for an oxygen spectrum with different threshold values applied to the data.
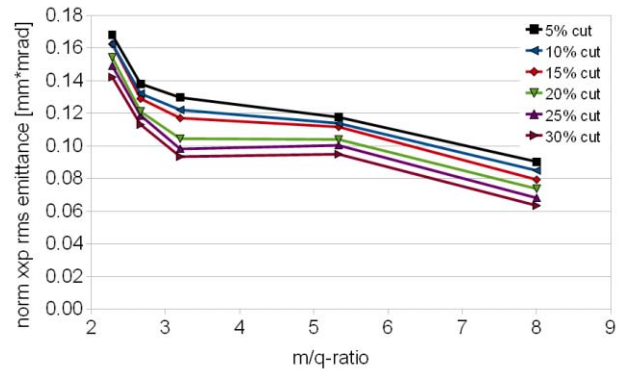

Figure 2: The emittance decreases as the noise threshold is increased and a greater portion of the spots is neglected. This change is different for every charge state and cannot be generalized.

For the top curve in figure 2 a 5% threshold was set, such that the spots on the pepper-pot image could just be separated and assigned to the corresponding holes. It can be clearly seen that for an increasing value of the threshold, the emittance becomes smaller.

Figure 3 shows the change of the emittance value for each charge state as the threshold is increased. The individual change for each charge state can be due to the fact that the intensity distribution in bigger spots is more diluted which results in a bigger intensity as the threshold cut is applied. As mentioned before, for future analysis the threshold cut must be replaced by a fitting routine in order to obtain even more realistic emittance values.
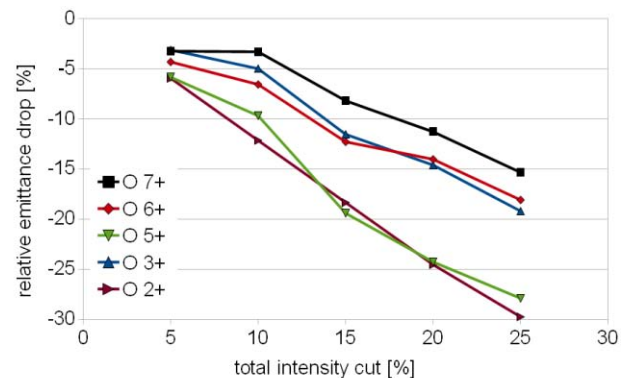

Figure 3: The difference in change of the emittance value for each charge state with different threshold values means that for bigger spots are the intensities are more diluted, resulting in a bigger decrease through the threshold cut.

DEVICE CALIBRATION

Since a pepper-pot scanner method is based on an optical data acquisition system, it is essential to investigate the influence of optical parameters such as the light response of the scintillating surface, the shutter time of the camera, the camera gain and the noise threshold on the obtained emittance values. Both the light yield of the scintillating surface as well as the shutter time of the camera determine the amount of light that falls onto the CCD chip. Therefore, these parameters play an important role for the sensitivity of the device. Previous measurements[1] have demonstrated that the light yield increases linearly with the deposited particle current and that the scintillator does not saturate in the tested current range. The next parameter to be considered is the camera gain. After the emittance pattern has been captured the gain is simply a multiplication of the image with a constant value. Generally, the gain and the shutter time should be chosen such that the CCD chip is close to its saturation in order to maximize the sensitivity of the measurement. The influence of each value is discussed in the following paragraphs.

The influence of the shutter time on the emittance value is shown in Figure 4, in which the emittance value is plotted as a function of the exposure time of the CCD chip. The data were taken with the same ion beam (33 µA, O^{5+}, 10 keV), while the ion source and beam line settings were kept constant for the measurement. Obviously, the shutter time has to be chosen to fall in the flat region of Figure 4 in order to measure realistic emittance values. On the other hand, the shutter time must be small enough to avoid saturation of the the chip, which would cut off the top of the spots.
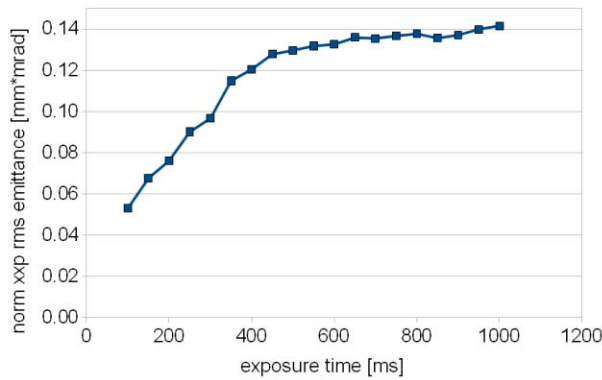

Figure 4: Generally, the spots become bigger as the shutter time increases. This induces a larger angular spread, which leads to a higher emittance.

As mentioned before, the gain of the camera is a constant value by which each pixel value is multiplied after the image has been captured. This increases image contrast, and the faint border regions of every spot become more visible as the gain is increased. However, this simple multiplication does not improve the signal-to-noise ratio (SNR). Figure 5 shows how the 1 rms normalized emittance of an O^{2+} beam (10 keV) behaves as the gain is increased while all other beam line and acquisition parameters remained the same. Again, measurements should be performed in the flat region of the curve.

As can be seen from Figures 4 and 5, the gain and shutter time have to be chosen carefully so that the CCD chip is close to its saturation in order to maximize the sensitivity and the signal-to-noise ratio. In addition, it is useful to combine pepper-pot measurements with an electrostatic type of emittance measurement such as the Allison scanner to have an independent cross check. By combining the higher resolution and better dynamic range of an electrostatic scanner with the 4D pepper-pot emittance scanner, the maximum information about the beam emittance can be obtained.
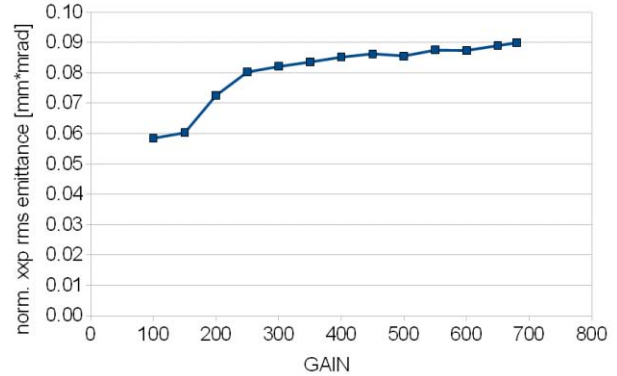

Figure 5: For small values of gain, the emittance appears to be very sensitive to changes in the camera gain. For a reliable measurement, the emittance value has to be evaluated from data taken in the flat region.

EMITTANCE VALUES OF ION BEAMS EXTRACTED FROM ECR ION SOURCES

The emittance of an ion beam extracted from an ECR source consists of two components: the magnetic emittance and the thermal emittance. For ECR sources, the magnetic influence is usually the main contribution to the total emittance and is influenced by the charge state of the ions and the axial field strength at the extraction aperture[5]. The ion temperature determines the thermal contribution to the emittance and is given by:

$$\varepsilon_{ther} = 0.016 \cdot R_{extr} \cdot \sqrt{\frac{kT_i}{M/Q}} \qquad (1)$$

where $R_{extr}[mm]$ is the radius of the extraction aperture, $kT_i \ [eV]$ is the ion energy and M/Q the mass-to-charge ratio. Accordingly, the magnetic contribution to the emittance can be calculated by:

$$\varepsilon_{mag} = 0.032 \cdot \left(R_{extr} \right)^2 \cdot \left(\frac{B_{extr}}{M/Q} \right) \qquad (2)$$

where $B_{extr} \ [T]$ is the maximum magnetic field at the extraction region of the source. For most ECR ion sources the magnetic component dominates over the thermal component [5].

EMITTANCE DATA

First emittance measurements with the new pepper-pot device were performed using the LBNL 6.4 GHz ECR and the 14 GHz AECR-U ion source.

1) Emittance change for different RF powers and beam intensities

As a first test, the beam emittance was measured as a function of the beam intensity. If more microwave power is coupled into the plasma, its density and consequently the beam intensity are increased, as long as the plasma remains stable. As an example, Figures 6 and 7 show a summary of a data series taken during a high intensity sulfur production run, where ECR source was optimized for S^{7+} through S^{10+}. The emittance values increase with increasing microwave power since the beam intensity for all charge states increases.

The average relative beam current increase of 30-40% between the different power levels is about the same as the increase in the absolute emittance values. Additionally, the plasma might be less stable at high power operation, which could lead to a higher emittance as well due to increasing transverse temperature. These two effects are difficult to decouple, but will be further investigated in the future.
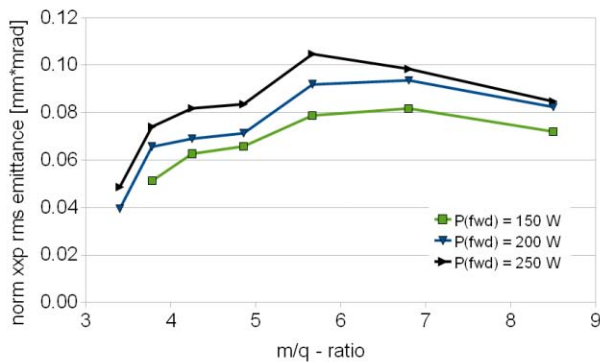

Figure 6: Coupling more RF power into the plasma increases the total extracted power and leads to an emittance growth.
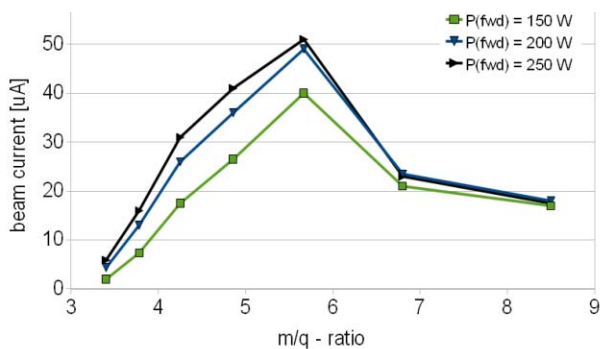

Figure 7: For high charge states the extracted current decreases, which makes the spots smaller, leading to a decreasing emittance number (see Fig. 6).

2) Emittance measurements at the ECR source

Figure 8 shows the result of a series of emittance measurements performed at the LBNL ECR ion source for oxygen, argon, sulfur and krypton beams extracted at 10 kV as a function of the mass-to-charge state ratio (m/q-ratio). For all data, the 1 rms normalized emittance

values are plotted after an intensity threshold cut of approximately 5%. It can be seen that for the same m/q-ratio heavier ions have a lower emittance than lighter ions, which is consistent with previous measurements[4]. This experimental result cannot be explained by equation 2 and might indicate that the particle distributions for heavier and lighter ions differ at the extraction aperture.

In addition, the measurements indicate a decreasing emittance for the higher charge states (e.g., Kr ions in figure 8). This could be an optical artifact since lower intensities are extracted for the higher charge states and the scanner might not be sensitive enough to measure the outer regions of the spots which would lead to smaller emittances. However, similar dependencies have been measured with Allison type slit scanners by various groups making the following interpretation possible as well. Due to the better confinement of the high charge states, the high charge state ions might be created closer to the axis of the source and would be extracted from a smaller region reducing the effect of the magnetic field on the transverse emittance.
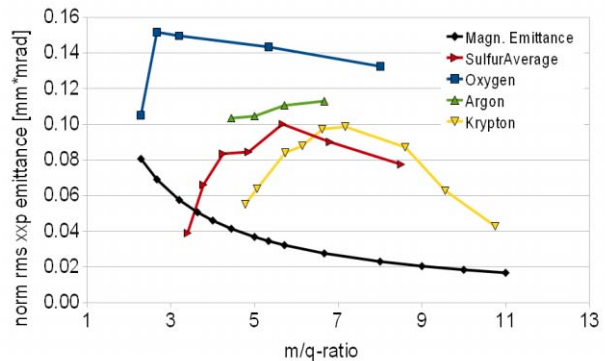

Figure 8: The data from the ECR source reveals that ions with a high mass have a lower emittance. This indicates a lower transverse ion temperature in the plasma.

3) Emittance measurements at the AECR-U source

A similar measurement series as described above for the LBNL ECR ion source was performed using the LBNL AECR-U ion source. Figure 9 shows the 1 rms normalized emittance for several species after an intensity threshold cut of about 5% was applied to the raw data. The extraction voltage was set to 12.5 kV and the maximum axial field strength in the extraction region is 0.9 T (about three times higher than the LBNL ECR ion source extraction field).

Contrary to the LBNL ECR source, most emittance values are well below the value predicted by the magnetic contribution (Equation 2), which indicates that the ion beam does not completely fill the extraction aperture. Similar to the ECR data, heavier masses have lower emittance values than lighter masses with the same magnetic rigidity. When the LBNL ECR ion beam emittance values are plotted together with the numbers obtained at the AECR-U ion source, the emittance values do not scale with the magnetic field as expected.
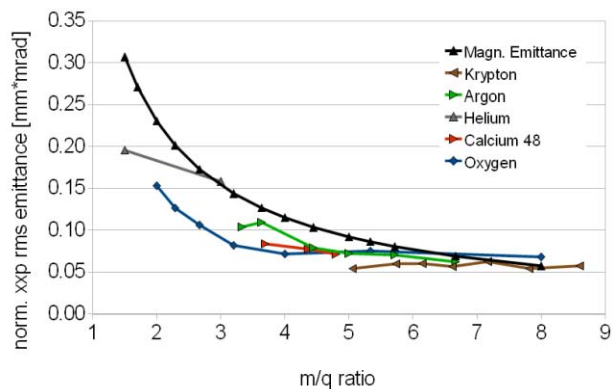
Figure 9: Especially for oxygen, the emittance grows clearly with the charge state and shows the same trend as the (theoretical) magnetic emittance.

Since the two analyzing beam lines are identical, any differences in the emittance values of the ion beams extracted from the two sources should only stem from the different magnetic field present at the extraction region. The maximum axial magnetic fields at extraction are 0.3 T for the LBNL ECR and 0.9 T for the LBNL AECR-U. The LBNL ECR emittance numbers should be three times smaller if the numbers would scale as predicted by Equation 2. The higher emittance measured at the LBNL ECR might be due to misalignment of the beam line or less stable plasma conditions and will be further investigated.

OUTLOOK

Future work with the LBNL pepper-pot emittance scanner will focus on comparing the results with an Allison type slit scanner and on further improvements of the analyzing software.

ACKNOWLEDGEMENTS

REFERENCES

[1] M. Strohmeier, J. Y. Benitez, D. Leitner, C. M. Lyneis, D. S. Todd, and M. Bantel. Rev. of Scientific Instruments, **81**, 02B710 (2010).

[2] S. A. Kondrashev, A. Barcikowski, B. Mustapha, P. N. Ostroumov, and N. Vinogradov, Nucl. Instrum. Methods Phys. Res. A **606**, 296 2009.

[3] H. R. Kremers, J. P. M Beijers, and S. Brandenburg, *A Versatile Emittance Meter and Profile Monitor* KVI, Groningen, 2007.

[4] D. Wutte, M. A. Leitner, and C. M. Lyneis, Phys. Scr. **T92**, 247 2001.

[5] M.A. Leitner, D.C. Wutte and C.M. Lyneis, *Design of the Extraction System of the Superconducting ECR Ion Source VENUS,* PAC2001 Proceedings, Chicago.